Supporting Information for: The Effect of a Receding Saline Lake (The Salton Sea) on Airborne Particulate Matter Composition

Alexander L. Frie [1], Justin H. Dingle[2], Samantha C. Ying[1,2], and Roya Bahreini[1,2*]

[1]Department of Environmental Sciences, University of California, Riverside, CA, 92521
[2]Environmental Toxicology Graduate Program, University of California, Riverside, CA 92521

[*]*Correspondence to:* Roya Bahreini (Roya.Bahreini@ucr.edu)
University of California, Riverside
900 University Ave.
Riverside, CA 92521
Tel: 951-827-4506
Fax: 951-827-4652

I. Supporting Text

Description of Trace Metal Digest Procedure

To determine total metal and metalloid concentrations, samples were placed in a Teflon vial, and 2.5 ml of concentrated HNO_3 and 0.5 ml of concentrated HF were added. All acids were sourced from Fisher Chemical and were trace metal grade or better. The closed vial was heated to 130-150 °C in an HEPA-filtered micro cleanroom, under negative pressure for 15 hours. While maintaining clean conditions, the vial was then uncapped and heated to 130 °C until ~0.5 ml of liquid remained. To assure total digestion of trace metals, 0.6 ml of concentrated HNO_3 and 1.8 ml of concentrated HCl were added to the vial for a second digestion. The closed vial was again heated on a hot plate to 130-150 °C for 15 hours. The vial was then uncapped and heated at 130 °C until ~0.5 ml of liquid remained. Finally, the solution was diluted with 2 ml of 5% HNO_3. The exact solution volume was determined by weighing the vial. The solution was transferred into an acid-cleaned 4 ml HDPE bottle and stored refrigerated until analysis.

An external geological standard (USGS G-2) was co-digested. For G-2, the relative method precision for all metals was better than 15%, while recovery of certified species, Na, Al, K, Ca, Mn, Fe was >79%. Co and Ba were the only certified species to display variation from the expected value by more than 21%. Lower than perfect mass recovery and some mass lost is expected as digests are known to have incomplete mass closure.[1] All aerosol data were blank corrected using elemental concentrations from the digested field blanks.

PM_{10} mass concentrations of each element are calculated by summing the elemental concentration of all digests (0.056 – 10 μm) for a specific aerosol sampling period. Filter digests resulting in values that were below the method detection limit (BDL) for specific elements were included unadjusted in PM_{10} mass concentrations, as replacement of a BDL value with "0" may skew the results. For a small subset of filter digests (6 of 129) where contamination occurred during preparation, the median value of each element within the same size range was used to replace the missing values when calculating PM_{10} mass concentrations.

Description of ED-XRF quantification

During ED-XRF analysis, United States Geologic Survey (USGS) standard reference material G-2 was also analyzed as an external standard. G-2 measurements were precise: all metals having an RSD of less than 7%. Variation from the expected value for certified species Na, Al, K, Ca, Fe was less than 30%. The only certified species to display error greater than 30% were Ti and Mn.

Positive Matrix Factorization Case Description

Three separate PMF models were run using concentrations of each element within PM_{10}, PM_{10-1}, and PM_1. Missing data values (6 out of 129 digests), removed due to contamination during digestion, were replaced with the

median value of the elemental mass concentration in that stage and given an uncertainty of 4 times this value. Below detection limit data were included to avoid introducing biases.[2] Internal PMF parameters, such as Q_{robust}, Q_{true}, and $Q_{expected}$ were considered to assess performance of PMF. In general, Q is a measure of the fitness of the model; Q_{robust} is calculated using only samples that fit the model well, while all samples are used in calculating Q_{true}. $Q_{expected}$ is equal to the number of samples multiplied by the number of strong species. The normalized contribution of each factor was constrained to above -0.2, and Q_{robust} was used per the settings of EPA PMF 5.0. Only results from the PM_{10} model data are reported here, as the PM_{10}, PM_{10-1} and PM_1 results were observed to be qualitatively similar. Ca, Na, As, Al Fe, Mn, V, Ba, Co, Se, Ti, K were classified as strong and Ni, Cd, Cr as weak species. Weak species were identified by a S/N ratio of less than 2; S/N ratios were calculated by PMF 5.0. Fpeak was set to 0 and no species were constrained to preset values. After running the model with 2-7 factors, a 4 factor solution was selected because of a low $Q_{true}/Q_{expected}$ (5.8) (Fig. S9), small residuals for most species and samples, absence of rotational ambiguity, and reasonable factor compositions. Within this solution, only Cd, Se, and Ba did not produce normally distributed residuals. Furthermore, only weak species displayed R^2 between distributions of observed vs. predicted values of < 0.6, and most strong species displayed R^2 values > 0.9, demonstrating the ability of this solution set to reproduce the sample data well. The uncertainty was estimated using the displacement method (Paatero et al., 2014). Bootstrapping was not used because of the small size of the sample set. High uncertainties were observed in the contribution of certain species to each factor, but each factor contained at least one well-constrained species, highlighting the dominant chemical characteristic of that factor. These high uncertainties stem, in part, from the high and variable values of field blanks that are carried through the model. Rotational swaps, indicating uncertainty in the identified components and their contributions, were not observed during displacement, and the largest change in Q was -0.01%, evidencing the good fit of the solution set.

Temperature Description

Ambient temperature (Fig. S2b) also displayed expected diurnal and seasonal variation, with the highest temperatures observed during summer afternoons and lowest temperatures observed during winter mornings. Average temperatures for BBS, SCS, and SCW at 06:00 LT (a proxy for the daily minimum temperature) were 31.8 °C, 31.6 °C, and 15.9 °C, respectively. Average temperatures for BBS, SCS, and SCW at 15:00 LT (a proxy for the daily maximum temperature) were 41.5 °C, 41.3 °C, and 29.7 °C, respectively.

Wind Direction Analysis

For SCS and BBS daytime wind values were well confined: during the day at SCS, greater than 60% occurrence of easterly winds (wind direction between 67.5° and 112.5°) was observed, while at BBS, wind direction

was predominantly southeasterly/southerly (wind direction between 112.5° and 202.5°). SCS and BBS night periods were more variable, with no octant having a probability greater than 35%. Despite this, BBS night wind directions varied primarily between southwesterly and southeasterly, with very low probabilities of northerly winds. SCW winds displayed the opposite diurnal variability trend, with night values having a dominant (90% probability) westerly wind direction (between 202.5° and 292.5°). No wind direction octant displayed greater than 25% probability during the day SCW periods.

References

1. Bettinelli, M., Beone, G. M., Spezia, S., and Baffi, C. Determination of heavy metals in soils and sediments by microwave-assisted digestion and inductively coupled plasma optical emission spectrometry analysis. *Anal. Chim. Acta* **2000**, 424, 289–296; DOI 10.1016/S0003-2670(00)01123-5
2. Brown, S. G., Eberly, S., Paatero, P., and Norris, G. A. Methods for estimating uncertainty in PMF solutions: examples with ambient air and water quality data and guidance on reporting PMF results. *Sci. Total Environ.* **2015**, 518–519, 626–635; DOI 10.1016/j.scitotenv.2015.01.022

II. Supporting Tables

Element	Average Desert, ppm	Average Playa, ppm	P Value, Playa vs Desert
Na	7.3e3 ± 3.3e3	7.2e4 ± 4.3e4	0.01
AL	4e4 ± 1.6e4	2.5e4 ± 8.2e3	0.04
K	1.4e4 ± 4.5e3	1.0e4 ± 2.5e3	0.04
Ca	2.9e4 ± 1.7e4	4.7e4 ± 1.4e4	0.02
Ti	3e4 ± 950	1.3e3 ± 460	0.00
V	55 ± 21	31 ± 14	0.02
Cr	31 ±13	18 ± 8	0.03
Mn	420 ± 180	210 ± 80	0.01
Fe	1.7e4 ± 8.8e3	1.0e4 ± 5.6e3	0.09
Co	6 ± 3	3 ± 2	0.03
Ni	13 ± 7	8 ± 4	0.12
Cu	15 ± 9	16 ± 18	0.15
Zn	49 ± 22	33 ± 15	0.15
As	7 ± 5	5 ± 3	0.27
Se	0.1 ± 0.1	0.5 ± 0.3	0.01
Cd	0.2 ± 0.1	0.2 ± 0.1	0.53
Ba	520 ± 200	250 ± 40	0.00
Pb	14 ± 6	7 ± 2	0.00

Table S1. Average elemental concentrations of playa and desert soils samples as measured via ICP-MS. P values were calculated from a two tailed, heteroscedastic, student's T test between the desert and playa samples. P value less than or equal to 0.05 are highlighted.

Element	Average Desert, ppm	Average Playa, ppm	P Value, Playa vs Desert
Na	1.3e4 ± 5.e3	1.3e5 ± 8.3e4	0.00
Al	7.9e4 ± 1.2e4	5.2e4 ± 2.2e4	0.00
K	1.8e4 ± 2e3	1.2e4 ± 5e3	0.00
Ca	4.5e4 ± 9e3	5.9e4 ± 2.1e4	0.00
Ti	3.4e3 ± 1e3	1.8e3 ± 1e3	0.00
V	60 ± 20	50 ± 20	0.02
Cr	40 ± 10	20 ± 20	0.00
Mn	410 ± 100	250 ± 150	0.00
Fe	2.4e4 ± 6e3	1.5e4 ± 1.0e4	0.00
Co	50%<BDL	50%<BDL	NA
Zn	50 ± 20	40 ± 20	0.00
As	50%<BDL	10 ± 20	0.95
Se	50%<BDL	2 ± 2	0.00
Cd	50%<BDL	50%<BDL	NA
Pb	23 ± 5	15 ± 5	0.00

Table S2. Average elemental concentrations of playa and desert soils samples as measured via ED-XRF. P values were calculated from a two tailed, heteroscedastic, student's T test between the desert and playa samples. P value less than or equal to 0.05 are highlighted.

Element	Median, PM$_{10}$, ng m^{-1}	Summer PM$_{10}$, ng m^{-1}	Winter PM$_{10}$, ng m^{-1}	Cal EPA Reference Exposure Levels, ng m^{-1}	P Value Summer vs.Winter
Na	480	850 ± 690	370 ± 160	NA	0.02
Al	620	870 ± 580	1e3 ± 880	NA	0.69
K	280	380 ± 270	410 ± 280	NA	0.78
Ca	670	940 ± 1.0e3	1.4e3 ± 1.8e3	NA	0.43
Ti	44	63 ± 39	57 ± 46	NA	0.75
V	1.8	2.1 ± 1.3	1.9 ± 1.4	NA	0.64
Cr	9	12.4 ± 8.8	11.1 ± 9.8	200 (Cr VI)	0.74
Mn	9.2	13.2 ± 9.3	12.2 ± 8.7	90	0.78
Fe	390	600 ± 430	540 ± 410	NA	0.72
Co	0.3	0.4 ± 0.2	0.4 ± 0.3	NA	0.63
Ni	5.7	8 ± 4.7	8 ± 8.3	14	1.00
As	0.5	0.7 ± 0.7	0.4 ± 0.2	15	0.14
Se	0.9	2.2 ± 2.7	0.3 ± 0.4	20000	0.02
Cd	0.05	0.42 ± 1.01	0.06 ± 0.03	20	0.20
Ba	15	24 ± 19	16 ± 8	NA	0.19

Table S3. Median, seasonal average, and standard deviations of PM$_{10}$ elemental concentrations, as measured via ICP-MS. P values were calculated from a two tailed, heteroscedastic, student's T test between the summer and winter samples. P value less than or equal to 0.05 are highlighted.

Element	Median EF	Average Summer EF	Average Winter EF	P Value, Summer vs. Winter
Na	2.2	3 ± 0.79	1.7 ± 1.3	<mark>0.011</mark>
K	1.1	1.2 ± 0.33	1.3 ± 0.34	0.715
Ca	2.3	2.8 ± 2.7	2.5 ± 2.5	0.56
Ti	1.6	1.9 ± 0.66	1.5 ± 0.39	0.074
V	1.5	2.2 ± 1	1.7 ± 0.92	0.17
Cr	31	40 ± 33	30 ± 14	0.33
Mn	2.1	2.3 ± 0.36	2.1 ± 0.99	0.5
Fe	1.6	1.7 ± 0.39	1.5 ± 0.55	0.33
Co	3	4.2 ± 3.1	2.9 ± 0.92	0.17
Ni	42	48 ± 28	39 ± 20	0.39
As	27	21 ± 12	21 ± 10	0.034
Se	1200	2200 ± 1200	400 ± 460	<mark>0.0001</mark>
Cd	64	610 ± 1400	61 ± 31	0.15
Ba	2.9	3.7 ± 3.7	2.5 ± 1.2	0.24

Table S4: Median, seasonal average, and standard deviation of PM_{10} EFs. P values were calculated from a two tailed, heteroscedastic, student's T test between the summer and winter samples. P values less than or equal to 0.05 are highlighted.
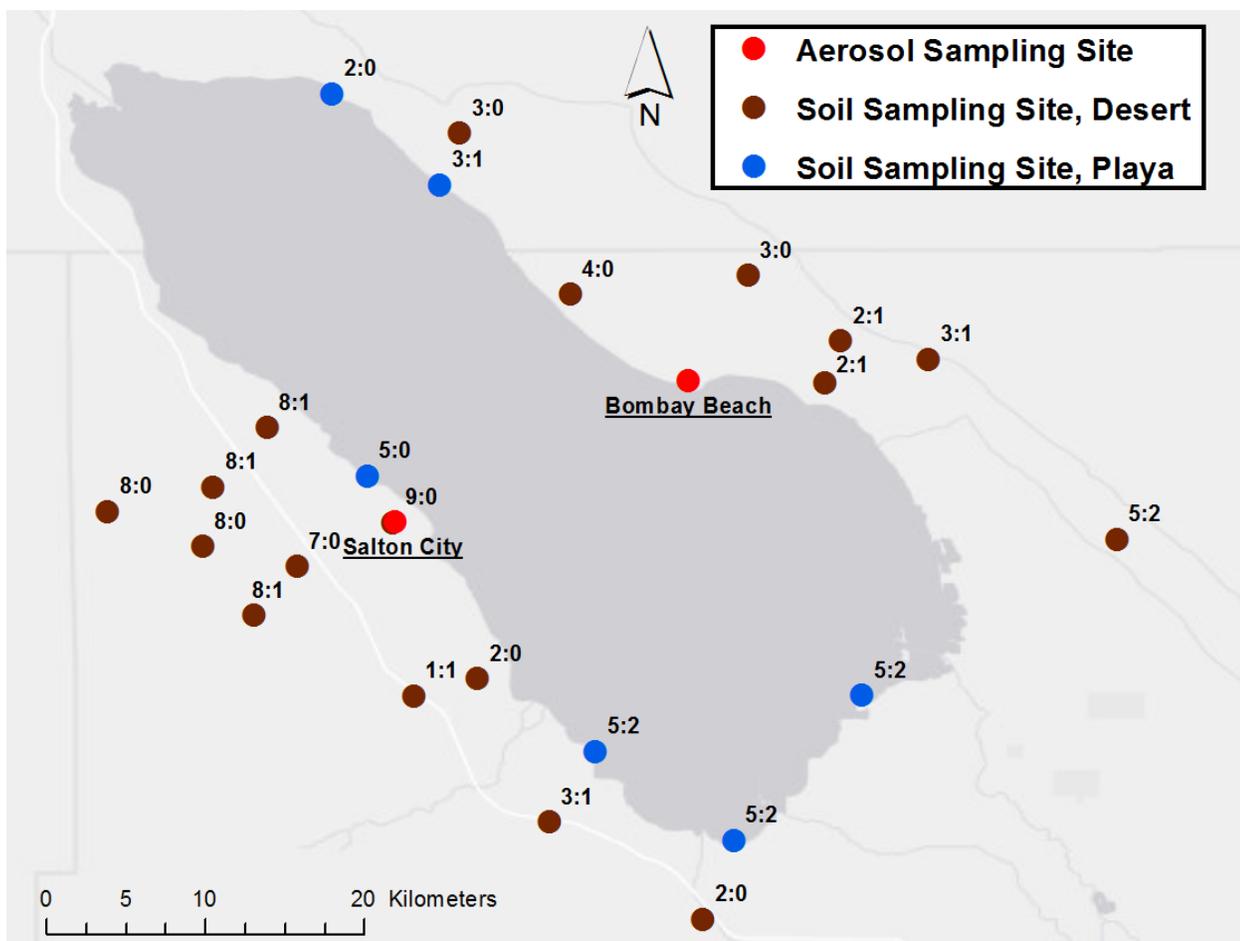
Figure S1. Map of soil and aerosol sampling sites. Labels represent the number of ED-XRF and ICP-MS analyzed soil samples from each site, presented as ED-XRF;ICP-MS.
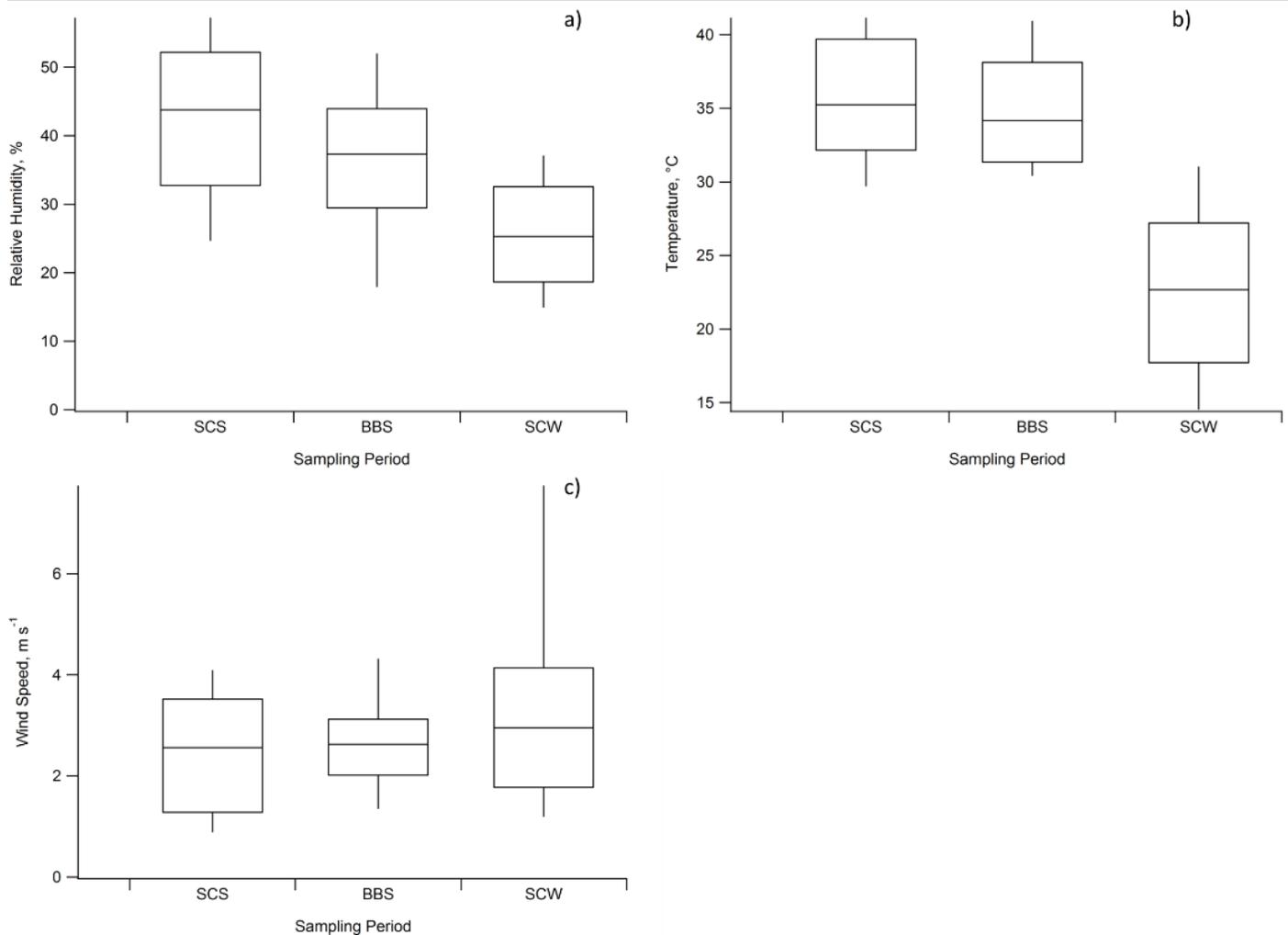
Figure S2. Meteorological data measured by the Imperial Irrigation District and downloaded from California's Air Quality Monitoring Information System Query Tool during aerosol sampling periods: Salton City Summer (SCS), Bombay Beach Summer (BBS), and Salton City Winter (SCW). Hourly averaged distributions of (a) relative humidity, (b) temperature, and (c) wind speed are reported. Box and whiskers highlight 10th, 25th, 50th, 75th, and 90th percentiles.
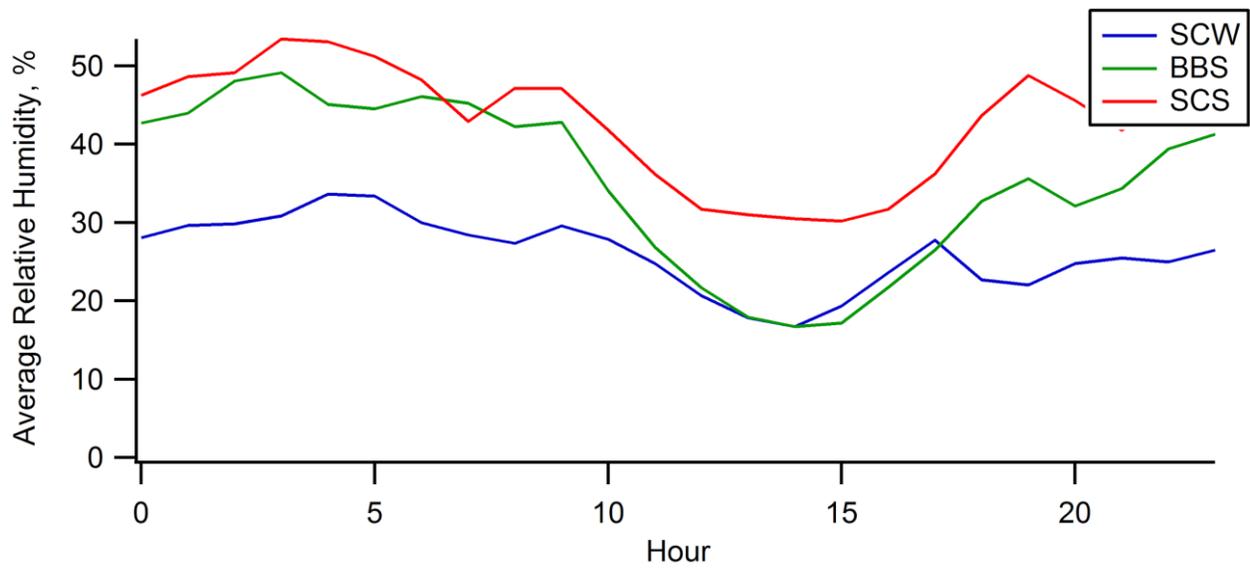
Figure S3: Average diurnal relative humidity pattern for Salton City Winter (SCW, Blue), Bombay Beach Summer (BBS, green), and Salton City Summer (SCS, red).
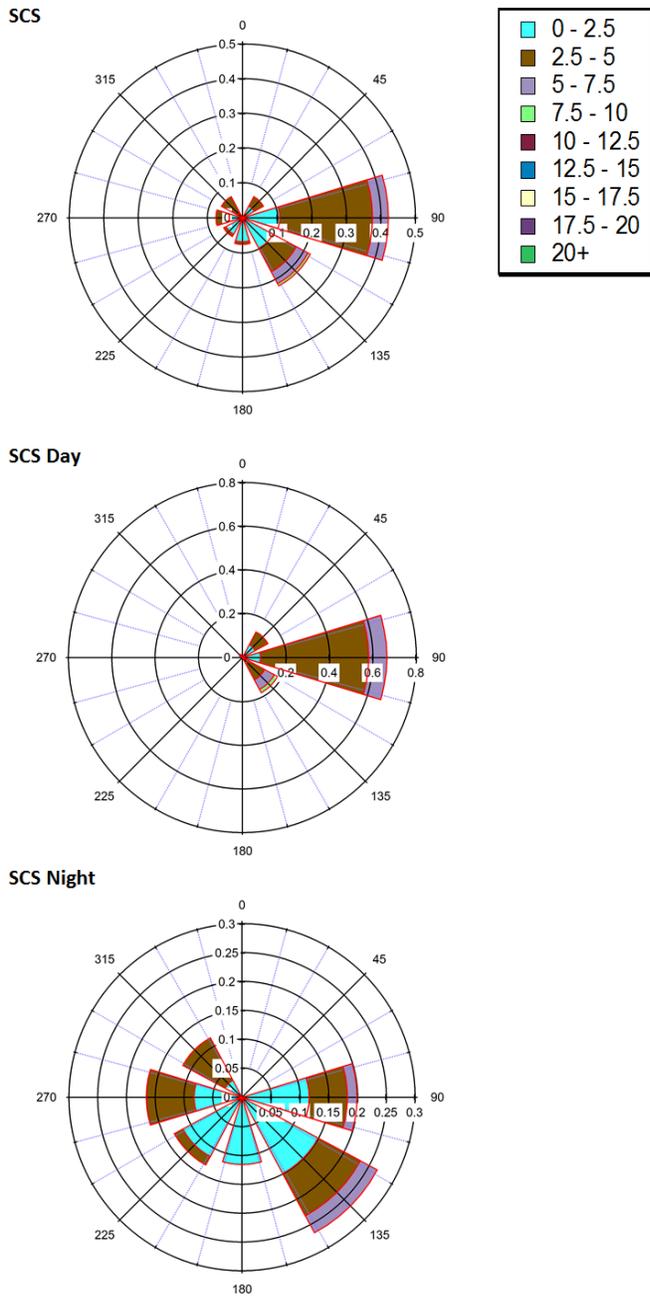
Figure S4: Wind Roses for Salton City Summer (SCS) sampling period. The probability of wind being sourced from a given direction is represented by the size of the colored portion and the colors represent wind speed probabilities in m s^{-1}.
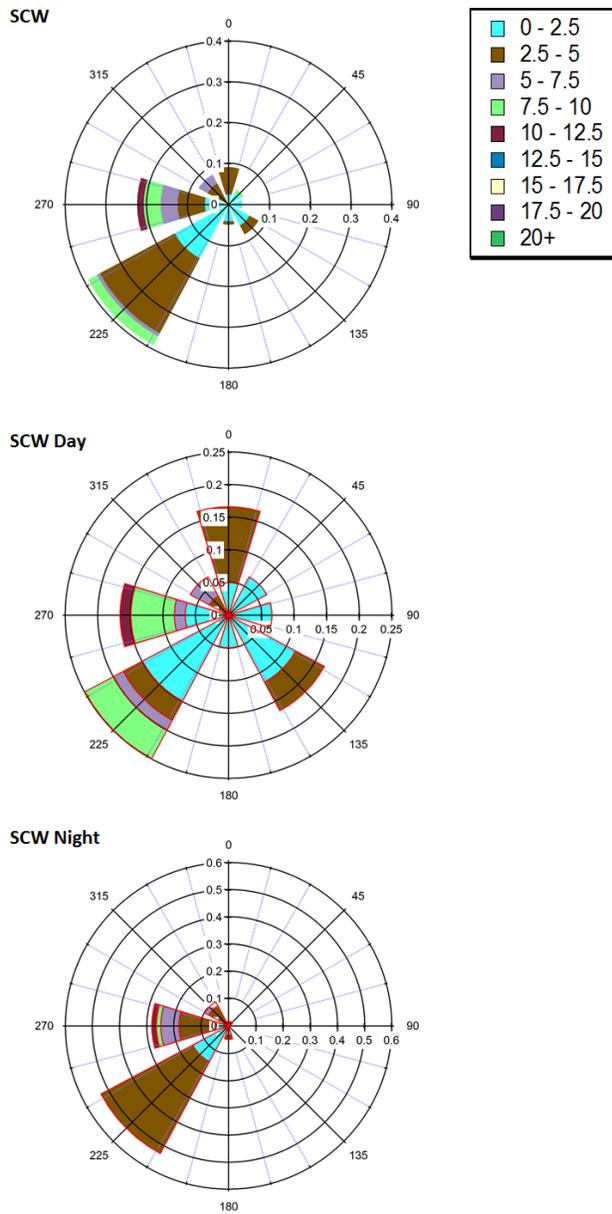
Figure S5: Wind Roses for Salton City Winter (SCW) sampling period. The probability of wind being sourced from a given direction is represented by the size of the colored portion and the colors represent wind speed probabilities in m s^{-1}.

BBS

BBS Day

BBS Night

Legend (wind speed, m s⁻¹):
- 0 - 2.5
- 2.5 - 5
- 5 - 7.5
- 7.5 - 10
- 10 - 12.5
- 12.5 - 15
- 15 - 17.5
- 17.5 - 20
- 20+
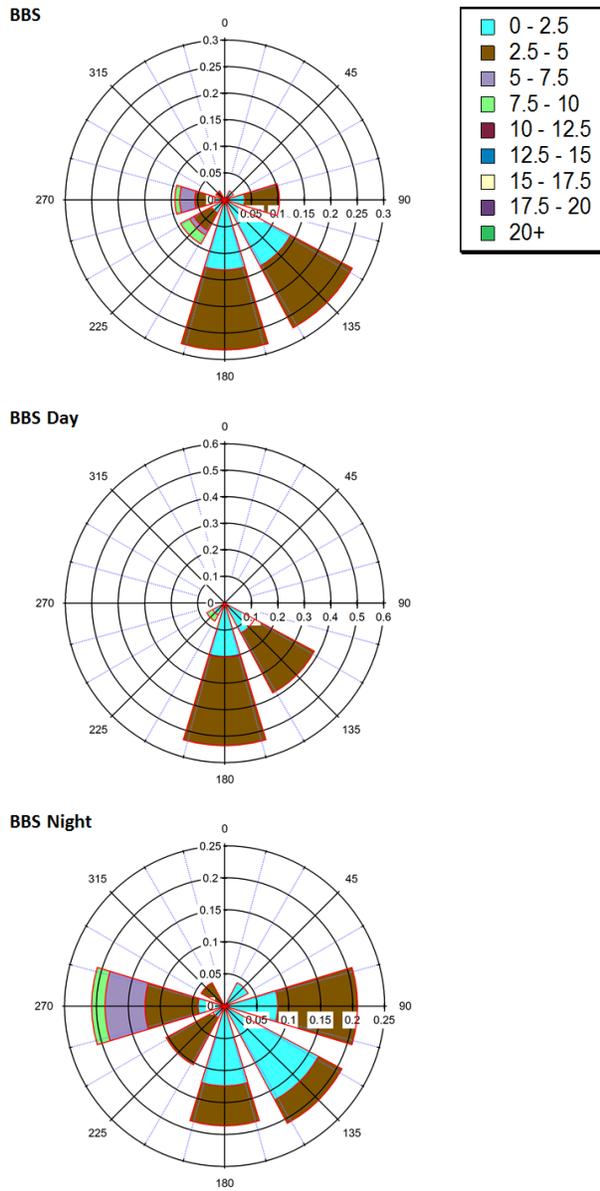
Figure S6: Wind Roses for Bombay Beach Summer (BBS) sampling period. The probability of wind being sourced from a given direction is represented by the size of the colored portion and the colors represent wind speed probabilities in m s^{-1}.
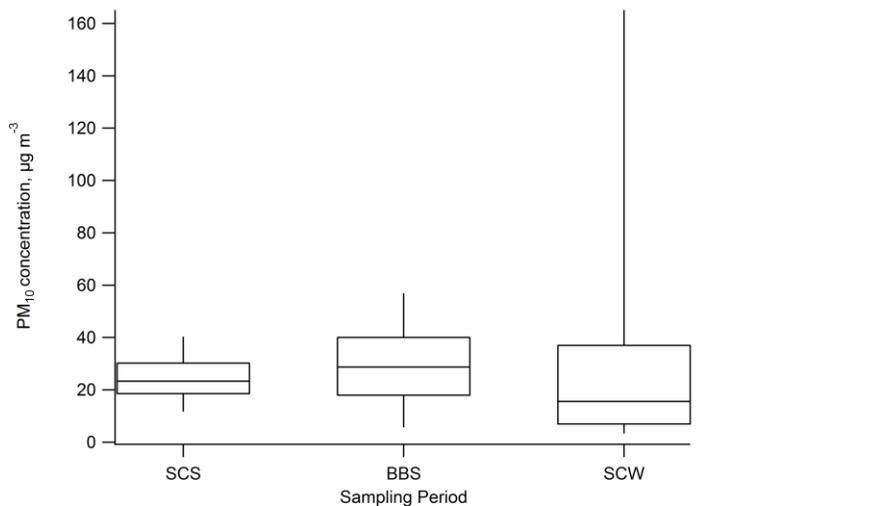
Figure S7. PM$_{10}$ mass concentration as measured by the Imperial Irrigation District and downloaded from California's Air Quality Monitoring Information System Query Tool during aerosol sampling periods: Salton City Summer (SCS), Bombay Beach Summer (BBS), and Salton City Winter (SCW). Box and whiskers highlight 10th, 25th, 50th, 75th, and 90th percentiles.
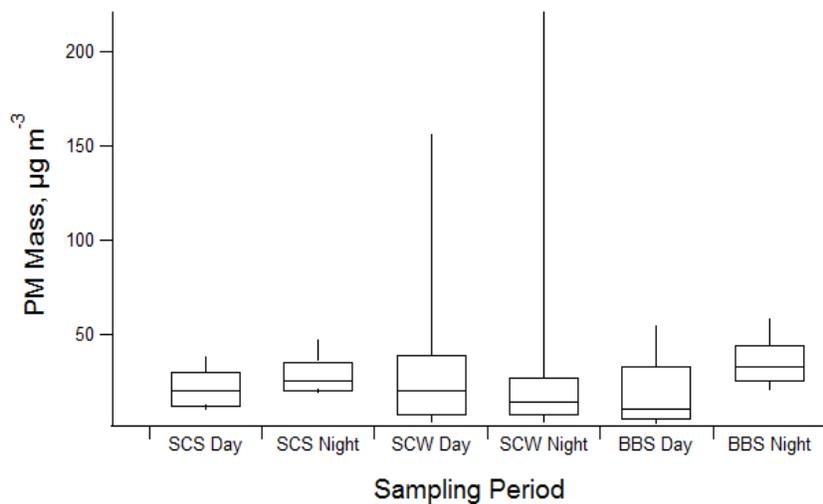
Figure S8. Diurnal PM$_{10}$ mass concentrations during Salton City Summer (SCS), Salton City Winter (SCW), and Bombay Beach Summer (BBS) sampling as measured by TEOM (Imperial Irrigation District, data available through the AQMIS).
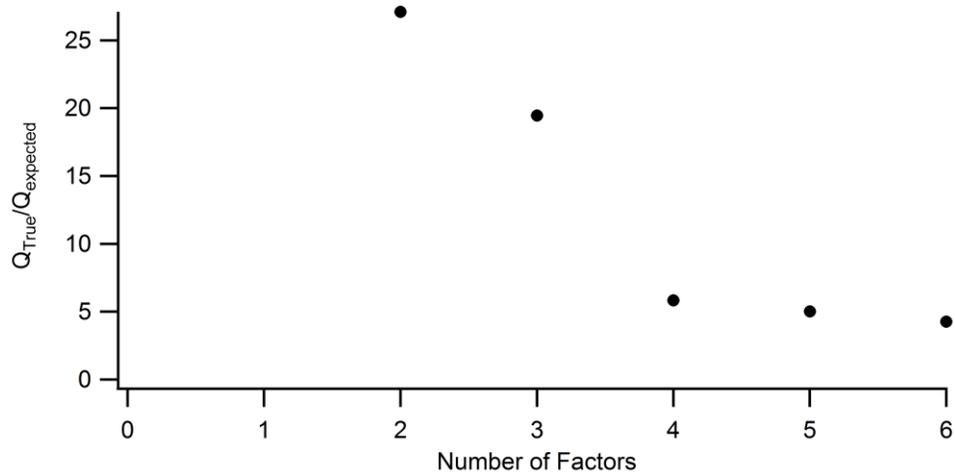
Figure S9. $Q_{true}/Q_{expected}$ ratio of positive matrix factorization results with different factor number inputs. A 4 factor model was selected as being the most accurate to describe the data because the change in $Q_{true}/Q_{expected}$ was insignificant after addition of another factor.